Quantum Electronics **43** (8) 762–767 (2013)

OPTICAL COHERENCE TOMOGRAPHY

PACS numbers: 42.25.Kb; 42.30.Wb; 87.63.L–; 42.79.Pw
DOI: 10.1070/QE2013v043n08ABEH014984

Enhancement of the resolution of full-field optical coherence tomography by using a colour image sensor

A.L. Kalyanov, V.V. Lychagov, I.V. Smirnov, V.P. Ryabukho

Abstract. **The influence of white balance in a colour image detector on the resolution of a full-field optical coherence tomograph (FFOCT) is studied. The change in the interference pulse width depending on the white balance tuning is estimated in the cases of a thermal radiation source (incandescent lamp) and a white light emitting diode. It is shown that by tuning white balance of the detector in a certain range, the FFOCT resolution can be increased by 20% as compared to the resolution, attained with the use of a monochrome detector.**

Keywords: *full-field interferometry, interferometry in white light, white balance, fill-field optical coherence tomography.*

1. Introduction

White light interferometry has been used for a long time (mainly as a technique of low-coherence interference microscopy) for measuring microscopic profile of surfaces and thickness of thin films [1, 2]. At present this method is being actively developed and finds application in the so called full-field tomography of layered structures and biological objects [3–8]. This has become possible due to the appearance of high-quality semiconductor matrix image sensors and the development of hardware for computer post-processing of digitised images.

The basic metrological advantages of low-coherence interference microscopy systems include high lateral and longitudinal (axial) spatial resolution. High lateral resolution is provided by using high-quality microscope objectives with relatively large numerical apertures. In the longitudinal direction with the use of microscope objectives with relatively small numerical aperture the high resolution is provided by the sufficiently wide effective frequency spectrum and, therefore, small temporal coherence length of the recorded radiation [9–13]. With microscope objectives having large numerical aperture and rather narrow frequency spectrum, the longitudinal resolution of full-field tomography systems is mainly determined by the width of the angular aperture of the optical field [4, 10, 12, 14–18] and, therefore, small longitudinal spatial coherence length of the optical field [19, 20]. The effects of the frequency spectrum width and the angular aperture width on the longitudinal resolution of a full-field tomography system are competing with each other.

As shown in Ref. [21], the width of the effective frequency spectrum is determined by the joint effect of all elements of the optical scheme, including the image sensor, on the radiation spectrum of the source. For a broadband radiation source (e.g., a thermal white light source) this effect can be essential and leads to significant narrowing of the resulting spectrum and, as a consequence, to the reduction of the system resolution. Assuming such elements of the optical system as mirrors, beam splitters and microscope objectives to be ideal from the point of view of spectral characteristics, the choice of an appropriate detector that has to possess sufficient sensitivity in a wide spectral range becomes a subject of primary importance.

As a rule, interference signals in full-field tomography are recorded using monochrome matrix image detectors, the sensitivity spectral range of which is essentially smaller than the spectral width of the radiation from thermal white light sources [5, 6, 11, 22] and exerts dominant influence on the effective spectral width of the recorded radiation. At the same time the shape of the interference pulse depends not only on the width of the spectral profile, but also on its shape, by variation of which one can achieve a certain narrowing of the interference pulse. This can be done by varying either the source spectrum, or the spectrum of the detector sensitivity. The first way was proposed in Ref. [23], where the broadband radiation was obtained from a combined source consisting of a few relatively narrowband quasi-monochromatic light emitting diodes emitting at different centre wavelengths.

In the resent paper we demonstrate the possibility of changing the effective spectrum of the recorded radiation by controlling the spectral sensitivity of the detector [24]. For this purpose it is proposed to use a colour image sensor. The filters of such a sensor are characterised by relatively narrow spectral transmission bands, so that in each colour channel of the digitised image a comparatively broad interference pulse is produced. The summation of colour channel leads to essential narrowing of this pulse. In this approach the transmission spectra of the filters are fixed, so that to obtain the required effective spectrum one has to change the energy ratio between the colour components in the total signal. This procedure is known as white balance correction. Traditionally, when using the colour image sensors for recording interference patterns in white light, the white balance is set to provide the maximal similarity of interference colours in the interference pattern observed with naked eye and the colour image recorded by the camera. This means that the white

A.L. Kalyanov, V.V. Lychagov, I.V. Smirnov N.G. Chernyshevskii Saratov State University, ul. Astrakhanskaya 83, 410012 Saratov, Russia; e-mail: kalyanoval@yandex.ru;
V.P.Ryabukho N.G. Chernyshevskii Saratov State University, ul. Astrakhanskaya 83, 410012 Saratov, Russia; Institute of Precision Mechanics and Control, Russian Academy of Sciences, ul. Rabochaya 24, 410028 Saratov, Russia

Received 14 September 2012; revision received 12 April 2013
Kvantovaya Elektronika **43** (8) 762–767 (2013)
Translated by V.L. Derbov

balance is adjusted to the colour temperature of the source, i.e., to the source emission spectrum. In this case, in the recorded image one can observe an achromatic interference fringe of the zero order (white or black). Otherwise, the achromatic fringe is absent; however, the width of the interference pulse envelope can appear to be smaller than in the case of adjusting the white balance to the colour temperature of the source.

In the present work we studied the effect of the white balance adjustment on the total interference signal recorded by the colour image sensor. The dependence of the interference pulse width on the weighting factors of the colour channels is shown. The possibility of increasing resolution of the interference system, as compared to the case of a detector with the white balance adjusted to the source emission spectrum, is demonstrated theoretically and experimentally.

2. Theory

2.1. Recording the interference signal with a colour detector

The effective spectrum of radiation $\tilde{S}_\mathrm{d}(\lambda)$ can be defined by the expression [21]

$$\tilde{S}_\mathrm{d}(\lambda) = S_\mathrm{d}(\lambda) S_\mathrm{s}(\lambda), \tag{1}$$

where $S_\mathrm{d}(\lambda)$ is the detector sensitivity spectrum; $S_\mathrm{s}(\lambda)$ is the emission spectrum recorded by the detector; λ is the wavelength.

According to the Wiener–Khinchin theorem [9], the temporal coherence function of such radiation can be presented in the form

$$\Gamma(\Delta) \sim \int_0^\infty \frac{1}{\lambda^2} \tilde{S}_\mathrm{d}(\lambda) \exp\left(\mathrm{i}\frac{2\pi}{\lambda}\Delta\right) \mathrm{d}\lambda, \tag{2}$$

where Δ is the optical path difference.

Knowing the sensitivity spectra $S_\mathrm{R}(\lambda)$, $S_\mathrm{G}(\lambda)$ and $S_\mathrm{B}(\lambda)$ of each colour channel, one can write the expression for the total sensitivity spectrum of the colour detector as

$$S_\mathrm{RGB}(\lambda) = \sum_{i=\mathrm{R,G,B}} S_i(\lambda). \tag{3}$$

With Eqns (1) and (3) taken into account, the expression for the total effective spectrum takes the form

$$\tilde{S}_\mathrm{RGB}(\lambda) = S_\mathrm{RGB}(\lambda) S_\mathrm{s}(\lambda) = \sum_{i=\mathrm{R,G,B}} \tilde{S}_i(\lambda), \tag{4}$$

where $\tilde{S}_\mathrm{R}(\lambda)$, $\tilde{S}_\mathrm{G}(\lambda)$ and $\tilde{S}_\mathrm{B}(\lambda)$ are the effective spectra of radiation that yields the interference signal in each colour channel of the detector. In order to account for the possibility of adjusting the white balance and, therefore, of controlling the total spectral sensitivity of the detector in the mathematical model of the interference signal formation, the weighting factors k_i should be introduced in expressions (3) and (4):

$$S'_\mathrm{RGB}(\lambda) = \sum_{i=\mathrm{R,G,B}} k_i S_i(\lambda), \tag{5}$$

$$\tilde{S}'_\mathrm{RGB}(\lambda) = \sum_{i=\mathrm{R,G,B}} k_i \tilde{S}_i(\lambda). \tag{6}$$

Here k_i is the factor of white balance for the corresponding colour channel.

From Eqns (2) and (6) it follows that the temporal coherence function of the radiation having the total effective spectrum (6) is equivalent to a weighted sum of coherence functions of radiation with the effective spectrum (1):

$$\begin{aligned}\Gamma_\mathrm{RGB}(\Delta) &= \sum_{i=\mathrm{R,G,B}} k_i \Gamma_i(\Delta) \\ &\approx \sum_{i=\mathrm{R,G,B}} k_i \int_0^\infty \frac{1}{\lambda^2} \tilde{S}_i(\lambda) \exp\left(\frac{\mathrm{i}2\pi\Delta}{\lambda}\right) \mathrm{d}\lambda \\ &= \int_0^\infty \frac{1}{\lambda^2} \tilde{S}'_\mathrm{RGB}(\lambda) \exp\left(\frac{\mathrm{i}2\pi\Delta}{\lambda}\right) \mathrm{d}\lambda.\end{aligned} \tag{7}$$

Figure 1a presents the sensitivity spectra of the detector colour channels with the transmission spectrum of the IR filter taken into account (matrix Sony ICX413AQ, camera Nikon D100, Japan) [25]. The spectra are normalised to make the area under curves equal. This means equal contributions of each channel to the resulting signal, the maximal amplitude

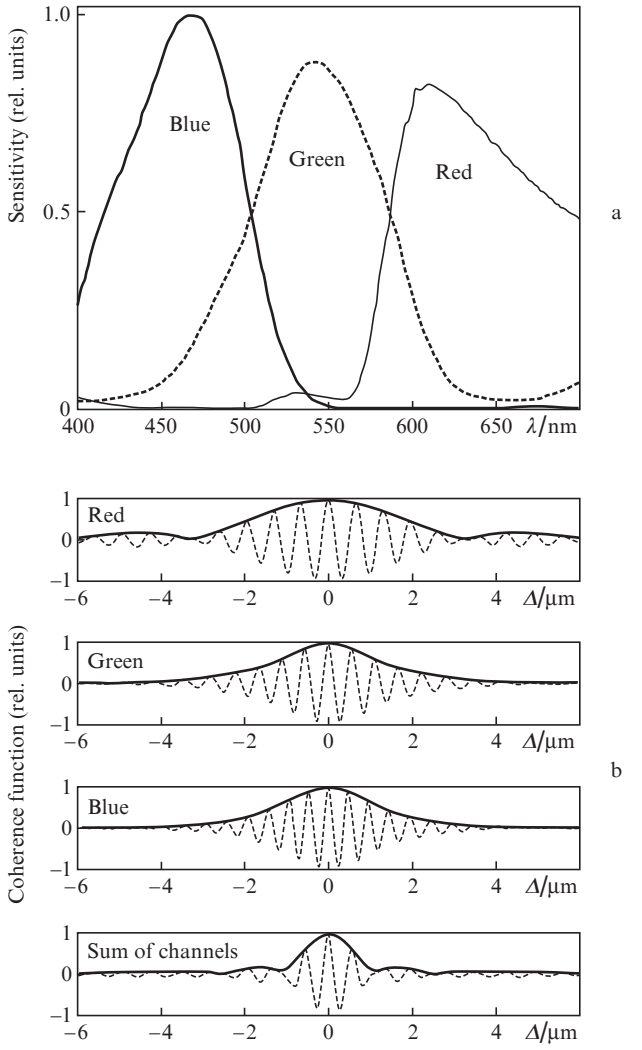

Figure 1. (a) Sensitivity spectra of colour channels in the Sony ICX413AQ matrix; (b) real parts and envelopes of coherence functions of the source with a uniform emission spectrum for each channel and their sum.

of the signal in each colour channel being dependent on the source radiation spectral composition only. Figure 1b shows the modelled real parts and envelopes of coherence functions for effective radiations in each colour channel recorded by such detector. The radiation source considered in the model had a uniform spectrum within the range of detector sensitivity. Figure 1b also presents the total coherence function and its envelope. The full width at half maximum of the coherence function envelope expressed in the optical path difference scale amounts to 3.7 μm for the red channel, 2.69 μm for the green channel and 2.62 μm for the blue channel. The width of the total coherence function equals 1.3 μm.

In the considered example the contributions of each colour channel to the total signal are equal and the correction of white balance is not required ($k_R = k_G = k_B = 1$). In the experiment it is difficult to provide such conditions because of the nonuniformity of the emission spectra from real sources and of the sensitivity spectra in semiconductor image sensors.

Figure 2 presents the effective radiation spectra in each colour channel of the detector. The sources used here were a white light emitting diode and a halogen incandescent lamp with the filament temperature 2700 K. From the ratio of signal amplitudes in the detector channels it is seen that for the incandescent lamp the red component is dominant, whereas for the white light emitting diode the blue and green components are dominant. The white balance correction consists in selective amplification of signals in individual channels. Thus, using the light emitting diode the signal should be increased by 2.5 times in the red channel and by 1.1 times in the blue one (Fig. 2).

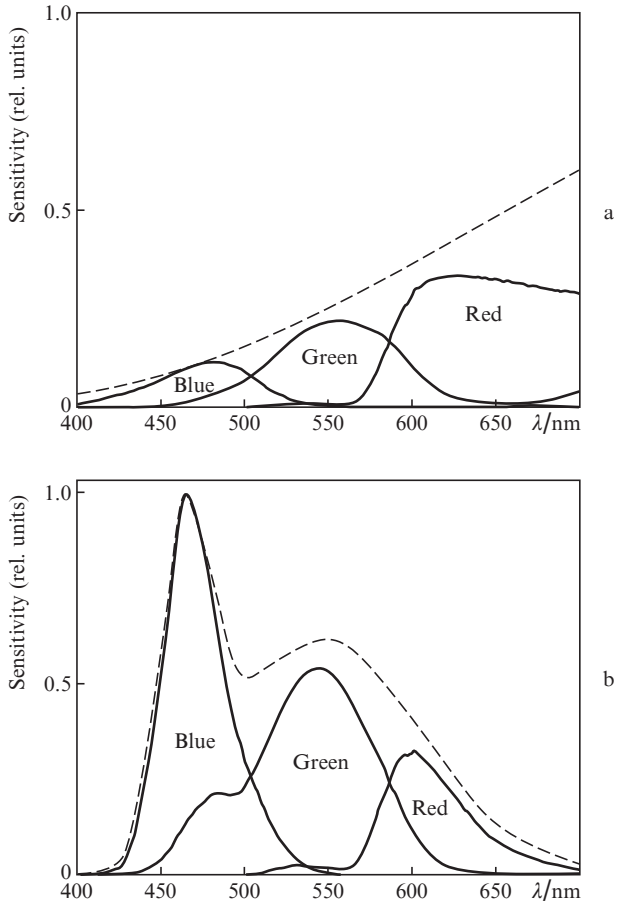

Figure 2. Source emission spectra (dashed curves) and corresponding effective emission spectra in colour channels of the detector (solid curves) for (a) a halogen incandescent lamp with the colour temperature 2700 K and (b) a white light emitting diode. The ratios of the signals in the blue, green, and red channels are (a) 0.2:0.6:1.0 and (b) 0.9:1.0:0.4, respectively.

2.2. Limits of variation for white balance factors

The range of variation for the white balance factors is largely dependent on the technical implementation of the procedure in a particular detector, as well as on the algorithms of further signal processing. In the present work two simplified rules were used:

1. The number of digits in the useful signal q_{sig} must exceed that of the noise q_{noise} at least by one. As a rule, the noise 'occupies' two–three lower-order ADC positions; for definiteness one can assume $q_{noise} = 2$. Then the present criterion can be formulated as:

$$q_{sig} \geqslant q_{noise} + 1 = 3. \tag{8}$$

2. The maximal value of the weighting factor should not exceed the number of discrete values of the signal level. Most of the modern image detectors are designed based on 12-bit matrices, so that

$$k_{max} \leqslant 2^{q_{ADC} - q_{sig}} = 2^9, \tag{9}$$

where q_{ADC} is the ADC number of digits.

3. Calculation of the interference signal at different white balance adjustments

The influence of the white balance adjustment of the detector was estimated by tracing the variation in the total interference pulse width at the half-maximum of its envelope. According to Eqn (7), for a particular radiation source and a particular detector the parameters of the envelope of the total coherence function depend only on the weighting factors that determine the contribution from each colour channel

$$G_s^{src}(k_R, k_G, k_B, \Delta) = k_R \Gamma_R^{src}(\Delta) + k_G \Gamma_G^{src}(\Delta) + k_B \Gamma_B^{src}(\Delta), \tag{10}$$

where $\Gamma_R^{src}(\Delta)$, $\Gamma_G^{src}(\Delta)$ and $\Gamma_B^{src}(\Delta)$ are the radiation coherence functions for the particular source (src), determined by the effective emission spectrum in each colour channel.

Thus, the width l^{src} of the interference pulse for the given source and detector is also a function of three variables, $l^{src}(k_R, k_G, k_B)$, where $k_{R,G,B} \in [1, 2^9]$, as follows from condition (9).

Since the function of three variables is hardly representable graphically, it is reasonable to deal with a function of two variables. For this purpose one can introduce the vector $\boldsymbol{k}' = (k'_R, k'_G = 1, k'_B)$, related to the vector $\boldsymbol{k} = (k_R, k_G, k_B)$ by the expression

$$\boldsymbol{k}' = \frac{\boldsymbol{k}}{k_G}. \tag{11}$$

In this case from condition (9) for the vector $\boldsymbol{k}'$ it follows that

$$\max(\boldsymbol{k}') = \frac{\max(\boldsymbol{k})}{\min(\boldsymbol{k})} \leqslant 2^{q_{ADC} - q_{sig}} = 2^9, \tag{12}$$

where $\max(\boldsymbol{k})$ and $\min(\boldsymbol{k})$ are the maximal and the minimal value of the weighting factors, respectively.

Taking conditions (8) and (12) into account, the relations for the weighting factors can be written as

$$\log_2 k'_{R,B} \in [-9;9],$$
$$\log_2 k'_G = 0, \qquad (13)$$
$$\log_2 |k'_R - k'_B| \leqslant 9.$$

According to Eqn (13), the interference pulse width can be represented as a function of two variables $l^{src}(k'_R, k'_G = 1, k'_B)$, thus covering all admissible values of the weighting factors.

Figure 3a shows the dependence of the interference pulse half-width l^{2700} on the adjustment of detector white balance. The incandescent lamp with the filament temperature 2700 K was used as a source. The triangles show the values of logarithms of the vector $\boldsymbol{k}'(k'_R, k'_G = 1, k'_B)$ components that correspond to adjusting white balance to the source colour temperatures in the range 1600–20000 K. The squares show the values of the components of $\boldsymbol{k}'_{wd}$, corresponding to white balance, adjusted to the radiation from the light emitting diode. The circles show the values of the components of $\boldsymbol{k}'_{min}$, at which the minimal width $l^{2700}_{min}(k'_R = 2^{5.6}, k'_G = 1, k'_B = 2^{7.8}) = 1.12$ μm of the interference pulse is achieved. Figure 3b presents the moduli and real parts of the total coherence function of the radiation from the thermal source with colour temperature 2700 K. Figure 3c shows the dependence of the interference pulse width l_{wd} on the adjustment of the detector white balance with the white light emitting diode used as a source of radiation, and Fig. 3d presents the moduli and the real parts of the corresponding total coherence function. In this case the minimal pulse width is $l^{wd}_{min}(k'_R = 2^{4.3}, k'_G = 1, k'_B = 2^{2.9}) = 1.43$ μm.

The presented results demonstrate the influence of white balance in a colour image detector on the shape and width of the interference pulse and, therefore, on the resolution of the interference system. As shown in Figs 3a and 3b for the halogen lamp, by choosing the weighting factors of colour channels one can achieve the reduction of the interference pulse width by 45% (from 2.05 to 1.12 μm) compared to the pulse width l^{2700}_{2700} for white balance, adjusted to the radiation source spectrum. For white light emitting diode (Fig. 3,c,d) it is possible to reduce the pulse width by 29% (from 2.05 to 1.44 μm).

Table 1 summarises the widths of the coherence function envelope for radiation from different sources, the interference signal being detected by means of the colour (l_{min}, l_{source}) image sensor Sony ICX413AQ, as well as by the monochrome detector Sony ICX204AL (camera DCU223M Thorlabs). The values of l_{min} correspond to the minimal width of the interference pulse, achieved by tuning the white balance of the detector, and l_{source} corresponds to the pulse width with the detector

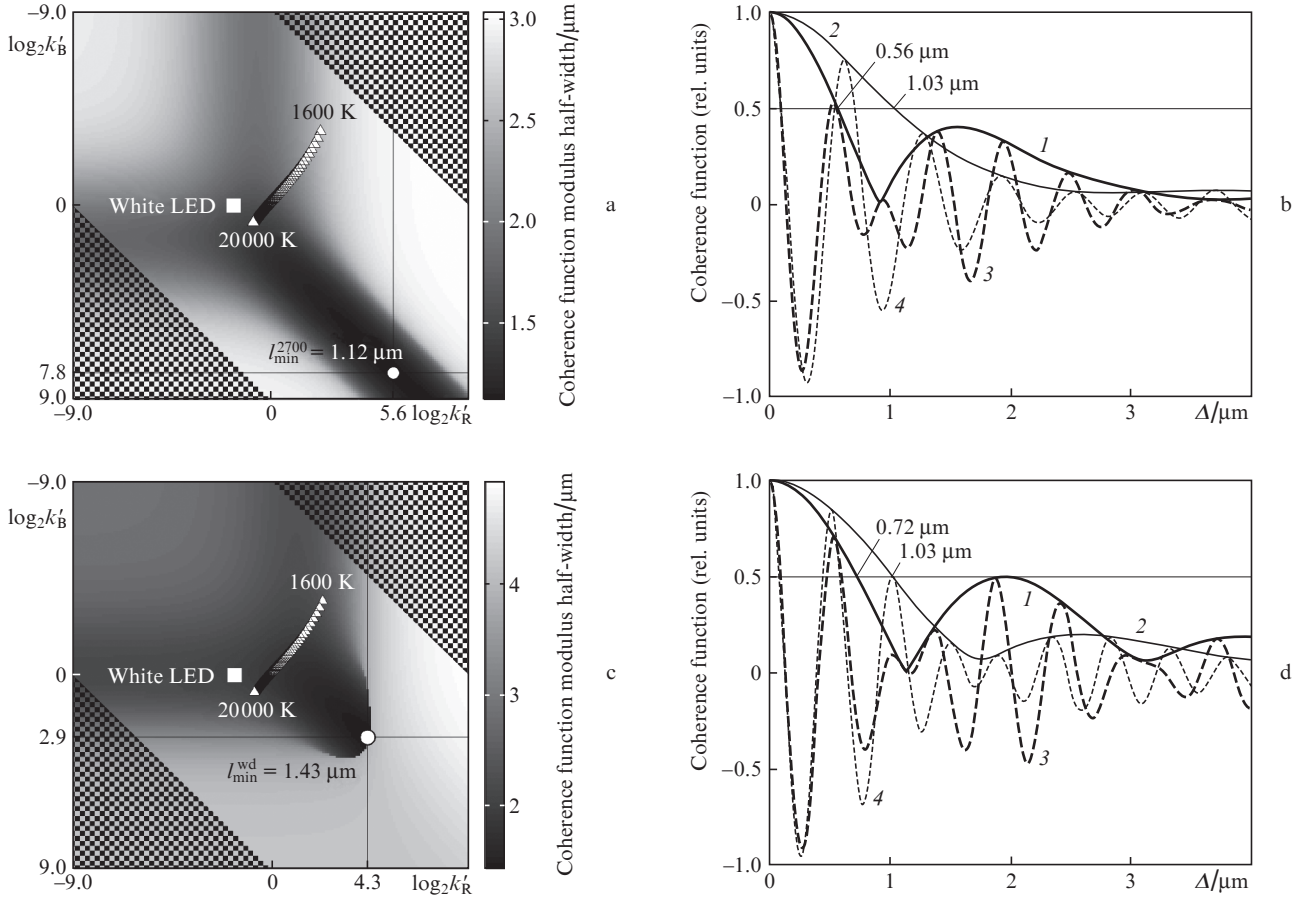

Figure 3. Dependences of the half-width of the coherence function modulus on the adjustment of the detector white balance using (a) the thermal radiation source with the colour temperature 2700 K and (c) the white light emitting diode; (*1*, *2*) moduli and (*3*, *4*) real parts of the total radiation coherence function for (b) the thermal source with the colour temperature 2700 K and (d) white light emitting diode. Curves (*1*, *3*) correspond to the minimal pulse width; curves (*2*, *4*) correspond to the pulse width in the case of white balance adjusted to the source emission spectrum.

Table 1. Full widths at half maximum of interference pulses for different radiation sources and detectors.

Radiation source	Interference pulse width/μm			$\log_2 k'_R$, $\log_2 k'_G$, $\log_2 k'_B$
	l_{min}	l_{source}	l_{mono}	
Incandescent lamp (2000 K)	1.14	2.49 (54%)	1.45 (21%)	4.4, 0, 8.0
Incandescent lamp (2700 K)	1.12	2.05 (45%)	1.31 (14%)	5.6, 0, 7.8
Incandescent lamp (3200 K)	1.12	1.89 (41%)	1.00 (–11%)	6.1, 0, 7.6
White light emitting diode	1.44	2.03 (29%)	1.82 (21%)	4.3, 0, 2.9

white balance adjusted to the source radiation spectrum. In brackets the reduction of the interference pulse width in percent is presented.

The monochrome detector Sony ICX204AL is sensitive within the spectral range 400–100 nm, which is essentially broader than the sensitivity range of the colour detector Sony ICX413AQ (400–700 nm), restricted with an IR filter. However, according to the data of Table 1, the use of the colour image detector allows an increase in the white light interferometer resolution even compared to that of a monochrome detector.

4. Experimental results

To test the theoretical results presented above, we performed an experiment on changing the interference pulse width by tuning the white balance of a colour detector. As a detector we used the digital photo camera Nikon D100 (Nikon, Japan). The data were stored and processed in the 12-bit RAW format.

The interference pattern was obtained in the Linnik microinterferometer MII-4 with the incandescent lamp having the colour temperature of 2700 K used as a source of light. A mirror was installed in the object arm of the interferometer. Figure 4a presents the normalised interference pulses recorded in each colour channel of the detector.

The white balance adjustment and the calculation of the total interference pulse were performed using Eqn (1) with Eqns (11) and (12) taken into account. Figure 4b shows the dependence of the interference pulse half-width on the white balance adjustment.

Despite a certain disagreement between the theoretical and experimental data, the obtained results clearly demonstrate the reduction of the interference pulse width from 1.83 μm [the point (0.0; 0.0) shown by a triangle in Fig. 4b] to 1.45 μm [the point (8.6; 9.0) shown by a circle in Fig. 4b], which amounts to 21%, as a result of adjusting the detector white balance. The pulse narrowing appears even more significant, than in the case of a signal, tuned to the white balance of the source. In this case the width of the interference signal amounts to 2.20 μm [the point (1; –1.4) shown by a square in Fig. 4b] and the pulse narrowing amounts to 34%.

5. Discussion and conclusions

In the low-coherence interference microscopy – the full-field tomographic microscopy – the longitudinal resolution is determined by the width of the produced interference pulse, which, in the case of using microscope objectives with relatively small numerical apertures, is inversely proportional to the width of the effective spectrum of the radiation producing the interference signal. In contrast to the interference methods that use laser radiation, in the case of using white light the effective spectrum is significantly affected by the sensitivity spectrum of the interference signal detector. The silicon monochrome image detectors widely used at present time allow implementation of the full-field white light interferometry providing the longitudinal resolution 1–2 μm.

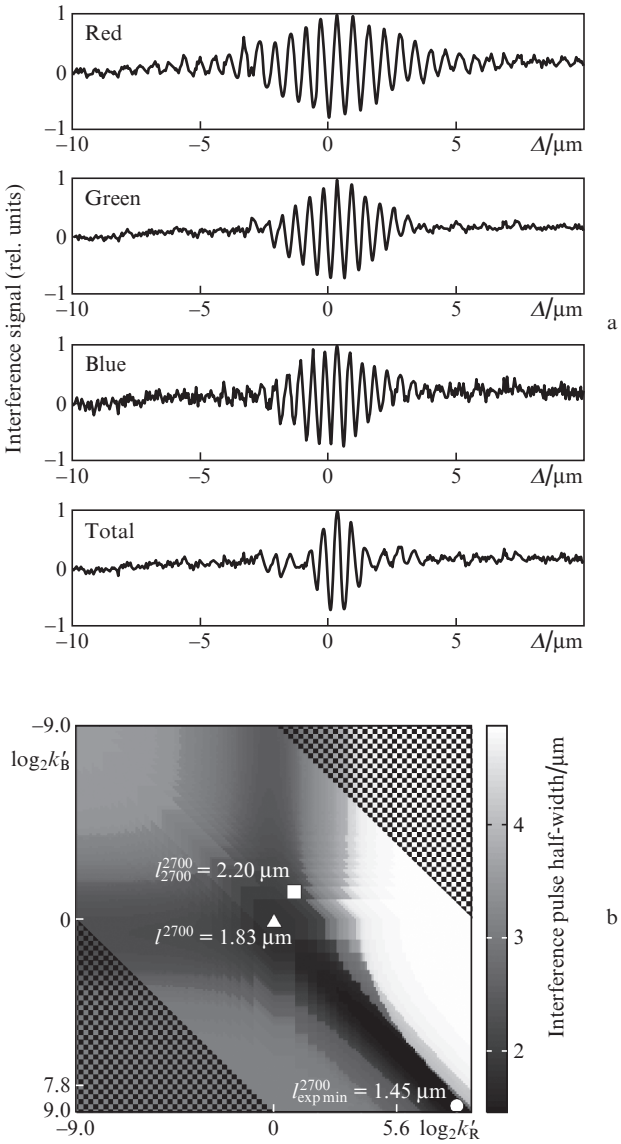

Figure 4. (a) Normalised interference pulses recorded in each colour channel of the Sony ICX413AQ detector and the total pulse, as well as (b) the dependence of the interference pulse half-width at the half-maximum level on the adjustment of the detector white balance. The source of radiation is the incandescent lamp (2700 K).

In contrast to the interference methods that use laser radiation, in the case of using white light the effective spectrum is significantly affected by the sensitivity spectrum of the interference signal detector. The silicon monochrome image detectors widely used at present time allow implementation of the full-field white light interferometry providing the longitudinal resolution 1–2 μm.

The use of monochrome detectors is inspired by the intension to obtain the maximal width of the effective spectrum. At the same time it imposes strict requirements on the optical components of the interference system, such as lenses, objectives and beamsplitters, since it is necessary to provide their spectral transparency within the entire range of detector sensitivity.

In the present paper we show theoretically and confirm experimentally that by varying the white balance in a full-field white light interferometer with a colour silicon detector it is possible to form an interference pulse having the width com-

parable with that obtained using a monochrome detector. The proposed approach allows the increase in the interferometer resolution without replacing the radiation source.

The comparison of the coherence function, having the minimum-width envelope due to white balance adjustment, with the interference pulses recorded with a monochrome detector and a colour detector with the white balance adjusted to the source radiation has demonstrated the possibility of increasing the device resolution in both cases (Table 1). Moreover, the application of a colour image detector allows the exploitation of the spectral range that is two times narrower than in the case of a monochrome detector, which softens the requirements to the optical elements of the interferometer.

The results of modelling have been confirmed experimentally. We believe that a certain difference between the measured and calculated data can be associated with a possible difference in the effective spectra of light sources used in the experiment and in the model, since we concede the presence of unrecorded influence of the interferometer optical elements on the effective radiation spectrum [26]. Another reason of a certain disagreement between the theory and the experiment may be the incorrect estimate of the permissible limits of variation in the weighting factors determined within the assumption that the interference pattern contrast is equal to one, which was not observed in the experiment (the interference pulses presented in Fig. 4 are normalised). In reality the contrast varied within the range 0.4–0.6 for different colour channels.

Despite the disagreements mentioned above, the performed experiment qualitatively confirms the possibility of changing the interference pulse width in full-field low-coherence interferometry by adjusting the white balance of a colour image detector.

Acknowledgements. The work was supported by the Ministry of Science and Education of the Russian Federation (Agreement Nos 14.B37.21.0728 and 14.B37.21.0563), the Russian Foundation for Basic Research (Grant No. 12-02-31204/12) and the President Grant for Government Support of the Leading Scientific Schools of the Russian Federation (Grant No. NSh-1177.2012.2).

References

1. Linnik V.P. *Dokl. Akad. Nauk SSSR*, **1**, 18 (1933) [*C. R. Acad. Sci. USSR*, **1**, 18 (1933)].
2. Deck L., de Groot P. *Appl. Opt.*, **33**, 31 (1994).
3. Beaurepaire E., Boccara A.C., Lebec M., Blanchot L., Saint-Jalmes H. *Opt. Lett.*, **23** (4), 244 (1998).
4. Dubois A., Vabre L., Boccara A.C., Beaurepaire E. *Appl. Opt.*, **41** (4), 805 (2002).
5. Grieve K., Dubois A., Simonutti M., Paques M., Sahel J., Gargasson J., Boccara C. *Opt. Express*, **13** (16), 6286 (2005).
6. Latrive A., Boccara C. *Biomed. Opt. Express*, **2** (10), 2897 (2011).
7. De Lega X., de Groot P. *Proc. SPIE Int. Soc. Opt. Eng.*, **6995**, 69950P (2008).
8. Binding J., Arous J., Léger J., Gigan S., Boccara C., Bourdieu L. *Opt. Express*, **19** (6), 4833 (2011).
9. Mandel L., Wolf E. *Optical Coherence and Quantum Optics* (Moscow: Fizmatlit, 2000, p. 896).
10. Dubois A., Grieve K., Moneron G., Lecaque R., Vabre L., Boccara C. *Appl. Opt.*, **43** (14), 2874 (2004).
11. De Groot P., de Lega X. *Appl. Opt.*, **43** (25), 4821 (2004).
12. Abdulhalim I. *J. Opt. A: Pure Appl. Opt.*, **8** (11), 952 (2006).
13. Sacchet D., Moreau J., Georges P., Dubois A. *Opt. Express*, **16** (24), 19434 (2008).
14. Dubois A., Boccara A.C., in *Optical Coherence Tomography. Technology and Applications* (Berlin: Springer, 2008) p. 565.
15. Zeylikovich I. *Appl. Opt.*, **47** (12), 2171 (2008).
16. Safrani A., Abdulhalim I. *Appl. Opt.*, **50** (18), 3021 (2011).
17. Safrani A., Abdulhalim I. *Opt. Lett.*, **37** (4), 458 (2012).
18. Abdulhalim I. *Ann. Phys.*, **524** (12), 787 (2012).
19. Ryabukho V.P., Lyakin D.V., Lychagov V.V. *Opt. Spektrosk.*, **107** (2), 296 (2009) [*Opt. Spectrosc.*, **107** (2), 282 (2009)].
20. Ryabukho V.P., Lyakin D.V., Grebenyuk A.A., Klykov S.S. *J. Opt.*, **15** (2), 025405 (2013).
21. Lychagov V.V., Ryabukho V.P., Kalyanov A.L., Smirnov I.V. *J. Opt.*, **14** (1), 015702 (2012).
22. Dubois A., Moreau J., Boccara C. *Opt. Express*, **16** (21), 17082 (2008).
23. Pakula A., Salbut L., in *Fringe 2009, 6th International Workshop on Advanced Optical Metrology* (Berlin: Springer-Verlag, 2009) pp 358–363.
24. Kalyanov A.L., Lychagov V.V., Ryabukho V.P., Smirnov I.V. *J. Opt.*, **14** (12), 125708 (2012).
25. http://www.alldatasheet.com/datasheet-pdf/pdf/222935/SONY/ICX413AQ.html.
26. Kalyanov A.L., Lychagov V.V., Smirnov I.V., Ryabukho V.P. *Izv. Saratov. Gos. Univer., Ser. Fiz.*, **11** (2), 19 (2011).